Characterization of Measured Indoor Off-Body MIMO Channels with Correlated Fading, Correlated Shadowing and Constant Path Loss

Patrick Van Torre, Luigi Vallozzi, Lennert Jacobs, *Student Member IEEE*, Hendrik Rogier, *Senior Member IEEE*, Marc Moeneclaey, *Fellow IEEE*, and Jo Verhaevert

Abstract—Indoor off-body wireless MIMO links between a mobile user equipped with wearable textile patch antennas and a fixed base station exhibit specific channel behavior due to the near presence and movements of the human body. Therefore, they require a dedicated channel model that captures the effects of correlated small-scale Rayleigh fading and correlated lognormal shadowing. A methodology is presented to construct such a model, allowing to predict the bit error characteristics and channel capacity curves based on the shadowing and fading correlation matrices that are extracted from channel measurements. It is shown that by separating shadowing, including effects caused by movement and reorientation of the human body, from small-scale fading, the main mechanisms of the off-body communication link are accurately captured by the model. A clear dependence of the shadowing correlation values on the physical layout of the antenna system is found. In our measurements, shadowing is not significantly decorrelated by polarization diversity or front-to-back diversity whereas the small-scale fading is clearly decorrelated. From the model, MIMO channel realizations with identical bit error rate and channel capacity characteristics as the measured channel can be quickly generated for link emulation purposes.

Index Terms—MIMO systems, MIMO channel, body-centric communications.

I. INTRODUCTION

WIRELESS off-body communication by means of textile antennas deployed in their garment is a convenient way to improve the safety and security of rescue workers. Important environmental and body parameters, measured by a system of sensors, are communicated in real-time to a command post. Reliable communication is of vital importance but when operating in an indoor environment, the reliability of the wireless link is compromised by small-scale fading and shadowing phenomena, among others.

When operating in an indoor environment characterized by Non Line-of-Sight (NLoS) radio propagation with Rayleigh distributed small-scale fading and lognormal shadowing, the use of multiple receive and/or transmit antennas drastically improves the reliability of the wireless link. Wearable textile antennas integrated into clothing allow a convenient implementation of multi-antenna systems onto the human body. The body area provides a large platform to deploy multiple antennas with sufficient separation to provide spatial diversity. In addition, the use of dual-polarized antennas doubles the number of exploitable signal paths for an equal number of antenna patches on the body; an additional doubling of the number of signal paths occurs when also the fixed access point is equipped with dual-polarized antennas.

A. Motivation

Characterization of the off-body MIMO channel is important for the development of suitable modulation and coding. In contrast to existing channel models available in literature, this paper proposes a dedicated channel model for:

1) Multiple flexible textile antennas exhibiting a directive radiation pattern, radiating away from the human body thanks to a ground plane.
2) Dual-polarized antennas directly deployed on the human body of a mobile user. Therefore the moving body will have a direct impact on the channel model. For example, wearable antennas positioned at the front and back sides of the body will exhibit significantly different correlation characteristics than omnidirectional antennas positioned in free space.

The proposed model is based on the separation of shadowing from small-scale fading, and is parameterized by a pair of independent correlation matrices for small-scale fading and shadowing, that are extracted from the channel measurements. This model allows the accurate generation of random MIMO channel realizations for simulation purposes.

B. Previous work

Multi-polarized MIMO channels have been studied thoroughly in [1], where an analytical model is presented, separating polarization effects from spatial effects. The additional effects of antenna rotation are documented in [2]. The use of a polarization metrics dependent adaptive codebook is outlined

in [3]. Polarization metrics are also used in [4], where the authors show that dual-polarized antennas can improve the performance of spatial multiplexing. Outdoor measurements and models for dual-polarized channels are documented in [5], however, with fixed antennas at both link ends.

Polarization metrics such as XPD (cross-polar discrimination) and CPR (co-polar ratio) are useful for links realized by means of fixed antennas [6], preferably in absence of moving scatterers. In the case of off-body communication with textile antennas [7], the antennas constantly change position and orientation. Additional fluctuations are introduced by body movements and bending of the antenna. XPD values are highly dependent on antenna orientation [2], limiting the relevance of average XPD values for this type of link.

Recent measurement campaigns related to body-centric wireless communication with multiple antennas have been described in [8]–[13]. These papers document the channel behavior, including signal correlation for multiple channels. A fading model is linked to the measurements in [14].

Signal correlation has an important impact on the performance of MIMO links. For indoor communication, signal correlation is caused by mutual coupling between antennas [15] and by the propagation environment [1]. Specific measurements for signal correlation in case of dual-polarized patch antennas are documented in [16].

Shadowing caused by obstacles in the environment also has an impact on the communication. Shadowing on different channels is also correlated and models for its behavior are documented in [17]–[20]. Measurements to determine the shadowing correlation are presented in [21].

C. Own contributions

In this paper, a new theoretical model is proposed for off-body communication links that communicate by means of textile antennas. Specifically it is shown that:

1) The channel behavior results from the combination of correlated fading and correlated shadowing effects, which are considered mutually independent. Unlike in [1] where polarization and spatial effects are separated, here the shadowing is separated from the small-scale fading. The channel model is accurately characterized by the shadowing and fading correlation matrices, with unequal average channel gain and unequal shadowing variances included.
2) Measured BER and capacity figures of merit are accurately reconstructed by the correlation model.
3) Channel realizations that exhibit identical properties as the measured channel can be emulated by means of the new model. An unlimited number of measurement-like MIMO channel realizations can be generated for the performance evaluation of modulation and coding under test.

D. Organization of the paper

The paper is organized as follows. Section II describes the setup for the channel measurement campaign. In section III, the observation model and the considered space-time codes are presented. Further, a MIMO channel model including lognormal shadowing and small-scale Rayleigh fading is introduced. The theoretical BER resulting from the considered MIMO channel is derived in terms of the shadowing and fading correlation matrices.

In Section IV, a method for estimating the elements of these correlation matrices based on channel measurements is proposed. Section V discusses the physical relevance of the extracted correlation values. Section VI indicates that the BER performance corresponding to the transmission of the considered space-time codes over the measured MIMO channel is closely approximated by the theoretical BER performance corresponding to the estimated correlation matrices. An additional validation of the channel model is obtained by comparing measured and modeled ergodic capacity curves in section VII.

II. CHANNEL MEASUREMENT SETUP

An experimental indoor off-body 2.45 GHz wireless MIMO link is investigated for NLoS channels. The path loss is assumed to be constant, as the rescue worker under test is operating at a large and fairly constant distance (17 m) from the transmitter, being the path depicted in red on Fig. 1. The direct signal path is blocked by brick walls, while, among others, metal closets and PC cases contribute to the shadowing.

Channel measurements are performed for a 4×4 MIMO configuration with the rescue worker wearing two dual-polarized textile antennas [22], on the front and back of the body, and walking at a speed of about 1 m/s. A similar set of antennas, which was readily available, is used at the fixed access point located at the other end of the link. The textile antennas with ground plane are efficient directional radiators, both when deployed on the body of a moving user and when used as fixed access point antennas. The dual-polarized patch antennas of the transmitter are mounted in the same plane at a given center-to-center distance. The TX antenna centers are separated by 10λ (122 cm) and 1.5λ (18 cm) in two subsequent measurement series.

The two measurement series are performed to illustrate the influence of the access point antenna separation on the shadowing correlation and the resulting bit error rate (BER) characteristic. The TX and RX antenna patches used are mounted such that they exhibit slanted cross-polarization $(+45°/-45°)$. However, when placed on the body, a rotation as well as a deformation of the polarization ellipses as a function of body posture is possible. The detailed behavior of the dual-polarized antennas in open space as well as on the human body is documented in [22].

The MIMO transmitter and receiver used are HaLo430 systems by Signalion, each equipped with four antenna ports. The receiver converts four RF signals to baseband. The baseband in-phase and quadrature signals are synchronously sampled, at a rate of 10 MHz. The samples are stored in local memory and are then transferred for further processing (using Matlab) to a PC by means of a USB-interface. The transmitter operates in exactly the reverse way, although the samples stored in local memory are now transmitted repetitively without reloading the data. However, the communication of data between the
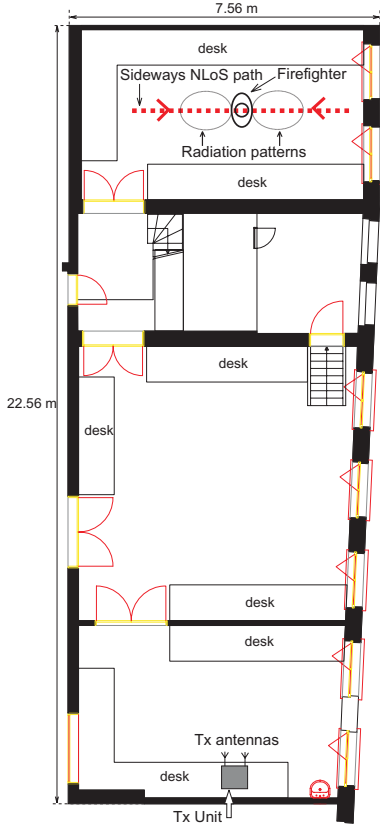
Fig. 1. Floor plan of the measurement environment, indicating the position of the transmitter and its antennas as well as the path walked by the firefighter.

HaLo430 system's internal memory and the PC is fairly slow and causes consecutive frames to be separated by a time interval of about 4 seconds. Although this causes the measurement to last a long time, the advantage is that the signals for the different captured frames are not temporally correlated. By letting the firefighter walk back and forth along the NLoS path for several hours, we collect a set of 2500 measured MIMO channel realizations, recorded at random positions along the path.

The channel measurements are obtained by sending bursts of 300 BPSK pilot symbols (of 1 μs duration each) from each transmit antenna in nonoverlapping time-slots. These pilot symbols are used at the receiver for time synchronization, frequency offset estimation and estimating the phase and amplitude of each SISO channel gain, which is assumed to be constant within a burst. In case of 4×4 MIMO communication, 16 SISO channels have to be estimated. We refer to [23] for a more extensive description of the transmission format and the channel estimation procedure.

III. SPACE-TIME CODING ON MIMO CHANNELS

A. Space-time codes

In MIMO transmissions, link quality can be improved by means of transmit and receive diversity using orthogonal space-time codes. In a space-time coded MIMO system with N_R receive and N_T transmit antenna ports, the received signal corresponding to a code word $\mathbf{C}$ can be represented by

$$\mathbf{R} = \mathbf{H}\mathbf{C} + \mathbf{W}, \tag{1}$$

where $\mathbf{R}$, $\mathbf{H}$, $\mathbf{C}$, and $\mathbf{W}$ are matrices of dimensions $N_R \times K$, $N_R \times N_T$, $N_T \times K$ and $N_R \times K$, respectively; with K equal to the number of time slots occupied by the codeword. The quantity $h_{m,n} = (\mathbf{H})_{m,n}$ is the complex channel gain between the m-th receive and n-th transmit antenna port; $\mathbf{C}$ is a space-time matrix with orthogonal rows (in case of orthogonal codes), whose elements are linear functions of L information symbols and their complex conjugates. The information symbols are assumed to be QPSK symbols, with variance σ_s^2. The elements of the noise matrix $\mathbf{W}$ are assumed to be i.i.d. complex-valued Gaussian random variables; their real and imaginary parts are independent and have equal variances $N_0/2$. The quantity $r_{m,k} = (\mathbf{R})_{m,k}$ denotes the signal captured by the m-th receive antenna port during the k-th time slot of duration T. In this paper, the performance of the Alamouti code [24] and the $3/4$ rate space-time code from [25, pp 194 (5.143)], will be investigated, when used on 2×2 and 4×4 links, respectively.

B. MIMO channel model

The effect of shadowing is very important in our transmission scenario. Position-dependent shadowing is caused by obstacles in the environment and orientation-dependent shadowing is caused by movements of the rescue worker, reorienting the on-body antennas' main beams. Unlike in [1], where polarization effects are separated from spatial effects, we propose a model isolating the shadowing from the small-scale fading. Shadowing and small-scale fading are assumed to be mutually independent.

When both shadowing and small-scale fading are present, the channel matrix $\mathbf{H}$ can be viewed as the element-wise product of a shadowing matrix $\mathbf{A}_{sh}$ (having positive elements) and a fading matrix $\mathbf{H}_{ss}$ (having complex elements), both of dimension $N_R \times N_T$. We define $\mathbf{h}$, $\boldsymbol{\alpha}_{sh}$ and $\mathbf{h}_{ss}$ as vectors of dimension $N_R N_T \times 1$ obtained by stacking the columns of the matrices $\mathbf{H}$, $\mathbf{A}_{sh}$ and $\mathbf{H}_{ss}$, respectively. Hence, $\mathbf{h}$ can be expressed as $\mathbf{h} = \mathbf{D}_{sh}\mathbf{h}_{ss}$, where $\mathbf{D}_{sh}$ is an $N_R N_T \times N_R N_T$ diagonal matrix with $(\mathbf{D}_{sh})_{i,i} = \alpha_{sh,i}$. Assuming small-scale Rayleigh fading, $\mathbf{h}_{ss}$ is complex Gaussian distributed with zero average and correlation matrix $\mathbf{R}_{ss} = E[\mathbf{h}_{ss}\mathbf{h}_{ss}^H]$.

For lognormal shadowing, the real quantities $\alpha_{\mathrm{dB},i} = 20log(\alpha_{sh,i})$ are Gaussian distributed with zero average and correlation matrix $\mathbf{R}_{\mathrm{dB}} = E[\boldsymbol{\alpha}_{\mathrm{dB}}\boldsymbol{\alpha}_{\mathrm{dB}}^T]$. When the fading and the shadowing are mutually independent, the correlation matrices $\mathbf{R}_{ss}$ and $\mathbf{R}_{\mathrm{dB}}$ completely characterize the MIMO channel statistics. Assuming that fading and shadowing are statistically independent, the resulting channel correlation matrix $\mathbf{R}_h = E[\mathbf{h}\mathbf{h}^H]$ is determined by

$$(\mathbf{R}_h)_{i,j} = (\mathbf{R}_{sh})_{i,j}(\mathbf{R}_{ss})_{i,j}, \tag{2}$$

where the correlation matrix $\mathbf{R}_{sh} = E[\boldsymbol{\alpha}_{sh}\boldsymbol{\alpha}_{sh}^T]$ can be computed from $\mathbf{R}_{\mathrm{dB}}$ as follows:

$$(\mathbf{R}_{sh})_{i,j} = E[\alpha_{sh,i}\alpha_{sh,j}] =$$

$$exp\left(\frac{1}{2} \cdot \frac{ln(10)}{10}^2 \cdot \frac{(\mathbf{R}_{\mathrm{dB}})_{i,i} + (\mathbf{R}_{\mathrm{dB}})_{j,j} + 2(\mathbf{R}_{\mathrm{dB}})_{i,j}}{4}\right). \tag{3}$$

C. BER performance

We now calculate the BER obtained when using a space-time code over the MIMO channel described in Section III-B and fully characterized by $\mathbf{R}_{dB}$ and $\mathbf{R}_{ss}$.

According to the observation model, the conditional BER for QPSK modulation with a given $\mathbf{h}$ is expressed as [26]

$$BER(\mathbf{h}) = Q\left(\sqrt{\frac{\sigma_s^2}{N_0}|\mathbf{h}|^2}\right). \qquad (4)$$

The average BER is obtained by averaging over the small-scale fading $\mathbf{h_{ss}}$ and shadowing $\boldsymbol{\alpha}_{sh}$. First, the averaging is performed over $\mathbf{h_{ss}}$ for a given $\mathbf{D}_{sh}$. For a given $\mathbf{D}_{sh}$, $\mathbf{h}$ represents Rayleigh fading with correlation matrix $\mathbf{D}_{sh}\mathbf{R}_{ss}\mathbf{D}_{sh}$. The result of averaging $BER(\mathbf{h})$ over the fading for a given shadowing realization is a function of σ_s^2/N_0 and $\mathbf{D}_{sh}\mathbf{R}_{ss}\mathbf{D}_{sh}$:

$$E_{\mathbf{h}_{ss}}[BER(\mathbf{D}_{sh}\mathbf{h}_{ss})] = g(\sigma_s^2/N_0; \mathbf{D}_{sh}\mathbf{R}_{ss}\mathbf{D}_{sh}). \qquad (5)$$

An analytical expression for $g(.;.)$ exists [27]–[29]. Subsequently, averaging is performed over the shadowing:

$$BER_{avg,th} = E_{\mathbf{D}_{sh}}[g(\sigma_s^2/N_0; \mathbf{D}_{sh}\mathbf{R}_{ss}\mathbf{D}_{sh})]. \qquad (6)$$

$BER_{avg,th}$ is the average BER corresponding to the theoretical channel model, characterized by $\mathbf{R}_{dB}$ and $\mathbf{R}_{ss}$. The averaging operator in (6) is calculated by means of Monte-Carlo integration:

$$BER_{avg,th} = \frac{1}{N}\sum_{n=1}^{N} g(\sigma_s^2/N_0; \mathbf{D}_{sh}(n)\mathbf{R}_{ss}\mathbf{D}_{sh}(n)). \qquad (7)$$

In this equation, $\mathbf{D}_{sh}(n)$ is a diagonal matrix defined as $(\mathbf{D}_{sh}(n))_{i,i} = 10^{\alpha_{dB,i}(n)/20}$, with $\boldsymbol{\alpha}_{dB}(n) = \mathbf{A}\mathbf{u}(n)$. The lower triangular matrix $\mathbf{A}$ results from the Cholesky decomposition of $\mathbf{R}_{dB} = \mathbf{A}\mathbf{A}^T$. The set $\{\mathbf{u}(n), n = 1, ..., N\}$ consists of N statistically independent realizations of a real Gaussian vector, with zero average and uncorrelated components with unit variance.

The performance indicator $BER_{avg,th}$ will be calculated as a function of E_b/N_0, with E_b the average energy per bit per receive antenna. For QPSK modulation and the considered space-time codes,

$$E_b = \frac{\sigma_s^2 \cdot E[|h|^2]}{2N_R} = \frac{\sigma_s^2 \cdot Tr(\mathbf{R}_h)}{2N_R}, \qquad (8)$$

with $\mathbf{R}_h$ calculated based on $\mathbf{R}_{dB}$ and $\mathbf{R}_{ss}$.

The theoretical error performance $BER_{avg,th}$ from (7) will be compared to the error performance $BER_{avg,meas.}$ that corresponds to the channel measurements. The latter is computed as

$$BER_{avg,meas.} = \frac{1}{M}\sum_{m=1}^{M} BER(\mathbf{h}(m)), \qquad (9)$$

with $BER(.)$ the conditional BER (4) and $\{\mathbf{h}(m), m = 1, ..., M\}$ a set of M channel measurements. The average received bit energy per receive antenna that corresponds to the measurements is given by

$$E_b = \frac{\sigma_s^2}{2N_R}\frac{1}{M}\sum_{m=1}^{M}|\mathbf{h}(m)|^2. \qquad (10)$$
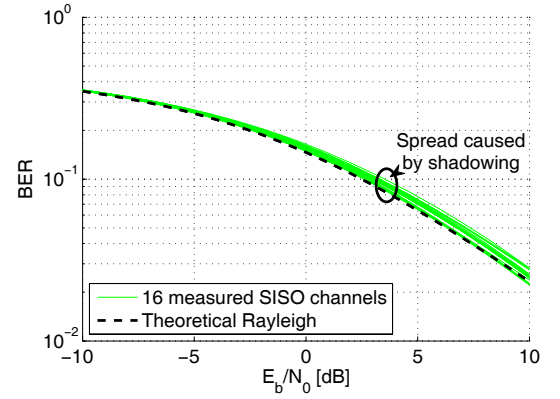

Fig. 2. BER characteristics for the measured SISO channels, displaying a shift to the right compared to the Rayleigh fading curve. This shift is caused by lognormal shadowing. E_b is the average energy per bit per receive antenna for the estimated SISO channel.

IV. PARAMETER EXTRACTION

A. Influence of shadowing on BER of SISO channel

We consider QPSK transmission on a SISO channel determined by a particular transmit and receive antenna. When N_T transmit antennas and N_R receive antennas are available, a total of $N_T N_R$ SISO channels can be considered. For each of these SISO channels, we compute the corresponding average BER (9) that results from the channel measurements. When computing (9), the vector $\mathbf{h}(m)$ reduces to a scalar $h_i(m)$, with i referring to the considered SISO channel.

Fig. 2 displays the BER characteristics for all 16 SISO channels corresponding to the measurement of an experimental 4×4 MIMO link in the case of indoor NLoS off-body communication (Section II, Fig. 1) with a pair of dual-polarized textile antennas and a base station equipped with similar antennas. The BER characteristics corresponding to Rayleigh fading curves have shifted to the right, depending on the amount of shadowing.

Although the shift of the characteristics appears minor for the SISO channels, the shadowing effects accumulate when these SISO channels are combined to create a MIMO channel.

In the case of Rayleigh fading without shadowing, the average BER on the SISO channel is proportional to $(E_b/N_0)^{-1}$ for large E_b/N_0 [26]. When shadowing is present, the BER averaged over the fading but conditioned on a shadowing realization α_{sh} is proportional to $\alpha_{sh}^{-2}(E_b/N_0)^{-1}$. Further averaging of the BER over the shadowing yields an expression that is still proportional to $(E_b/N_0)^{-1}$ for large E_b/N_0, because $E[\alpha_{sh}^{-2}]$ is finite when α_{sh} has a lognormal distribution. Consequently, for the SISO channels, lognormal shadowing does not influence the slope of the BER curve for high E_b/N_0 values but only causes a shift of the BER characteristic to higher E_b/N_0 values. This is confirmed by the behavior of the BER curves displayed in Fig. 2.

B. Estimation of the shadowing and fading variances

Now, we describe a procedure to estimate the shadowing standard deviation $\sigma_{dB,i}$ for the i-th SISO channel from channel measurements $\{h_i(m), m = 1, ..., M\}$.

TABLE I
SHADOWING FACTORS $\sigma_{dB}^{(i)}$ FOR THE 16 SISO CHANNELS COMPOSING
THE 4×4 MIMO LINKS WITH 10λ AND 1.5λ TX ANTENNA SEPARATION.
UNEQUAL AVERAGE CHANNEL GAIN ILLUSTRATED BY $10log(E[|h_i|^2])$
VALUES, NORMALIZED TO 0 dB FOR THE STRONGEST CHANNEL.

TX ant.	RX ant.	$10log(E[|h_i|^2])$ 10λ	$\sigma_{dB}^{(i)}$	$10log(E[|h_i|^2])$ 1.5λ	$\sigma_{dB}^{(i)}$
1	1	-1.6059	2.1584	-2.4898	1.4385
1	2	-1.9405	1.7713	-1.4675	3.3456
1	3	-4.6638	2.0962	-7.1399	3.8046
1	4	-2.8610	1.5815	-2.9732	1.2774
2	1	-0.4957	2.3589	0	3.6634
2	2	-0.8068	0.5304	-0.9383	2.2557
2	3	-4.5796	1.5501	-7.2706	2.5974
2	4	-0.5549	1.7198	-0.9591	3.9298
3	1	-0.1340	2.0013	-0.3374	1.2791
3	2	0	1.155	-1.4767	1.0524
3	3	-3.4440	1.7413	-7.8415	1.1525
3	4	-0.2739	1.6356	-2.5750	0.7179
4	1	-1.4143	2.0036	-3.4653	0.7280
4	2	-1.6455	0.6695	-1.5893	1.5102
4	3	-5.0189	1.3132	-8.4081	0.9396
4	4	-2.4016	0.0998	-4.1365	1.1217

Let us consider a trial value $\sigma_{dB}^{(i)}$ of the shadowing standard deviation for the i-th SISO channel. The corresponding small-scale fading variance $(\mathbf{R}_{ss})_{i,i} = (\sigma_{ss}^{(i)})^2$ that is consistent with the measurements $\{h_i(m), m = 1, ..., M\}$ is determined from

$$(\mathbf{R}_{sh})_{i,i}(\mathbf{R}_{ss})_{i,i} = \frac{1}{M}\sum_{m=1}^{M}|h_i(m)|^2, \qquad (11)$$

where $(\mathbf{R}_{sh})_{i,i} = E[\alpha_{sh,i}^2]$ can be computed from $\sigma_{dB}^{(i)}$ (3).

We define the modeling error $E_1(\sigma_{dB}^{(i)})$ related to the trial value $\sigma_{dB}^{(i)}$ as the squared error between $ln(BER_{avg,meas}^{(i)})$ and $ln(BER_{avg,th}^{(i)})$, averaged over some interval of E_b/N_0; here we consider 51 values of E_b/N_0 ranging from 0 dB to 5 dB, with an increment of 0.1 dB. In the above, $BER_{avg,meas}^{(i)}$ is the average BER (9) of the i-th SISO channel that corresponds to the measurements $\{h_i(m), m = 1, ..., M\}$, and $BER_{avg,th}^{(i)}$ is the theoretical average BER (7) of a SISO channel described by a shadowing standard deviation and fading variance $(\mathbf{R}_{ss})_{i,i}$ (which is related to $\sigma_{dB}^{(i)}$ by (11)). The shadowing variance estimate equals the trial value $\sigma_{dB}^{(i)}$ that minimizes $E_1(\sigma_{dB}^{(i)})$.

For E_b/N_0 values lower than 0 dB the influence of the estimated parameter on the characteristic is limited. Characteristics can be calculated starting from arbitrarily low E_b/N_0 values. Including the lower E_b/N_0 range for the parameter extraction does not significantly change the results. To limit the calculation time for the parameter extraction, the low end was chosen at 0 dB. E_b/N_0 values higher than 5 dB are not used in $E_1(\sigma_{dB}^{(i)})$ as the finite set of channel measurements (in our experiment, the number M of measurements per SISO channel equals 2500) limits the accuracy of $BER_{avg,meas}^{(i)}$ for these values of E_b/N_0.

The shadowing standard deviation estimates found for the SISO channels composing the measured 4×4 MIMO links with 10λ and 1.5λ TX antenna separation are shown in Table I.

The parameters for the shadowing of the SISO channels are important for the calculation of the BER for the MIMO channels composed by these SISO channels. In addition, as
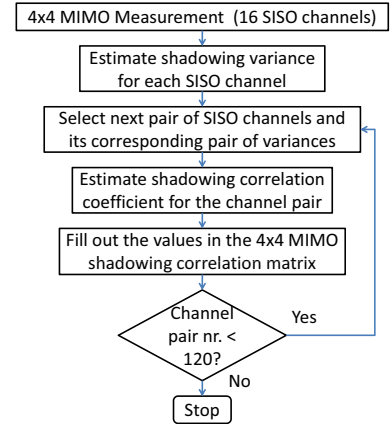

Fig. 3. Flowchart of the shadowing estimation procedure, determining the correlation coefficients for all 120 possible combinations of 2 out of 16 measured SISO channels.

the shadowing for different antennas is not independent, the correlation between the shadowing of the SISO channels should also be considered.

C. Estimation of the shadowing and fading cross-correlations

Once the shadowing standard deviations (or variances) of the SISO channels have been estimated, the shadowing correlation between different SISO channels is estimated. Fig. 3 displays a flowchart of the procedure for the shadowing correlation estimation.

Consider a pair (h_i, h_j) of SISO channels ($i \neq j$). For i and j ranging from 1 to 16, the number of pairs to be considered is $16 \times 15/2 = 120$. The shadowing correlation $\rho_{dB}^{(i,j)}$ and the fading correlation $\rho_{ss}^{(i,j)}$ between the considered channels are defined through the relations $(\mathbf{R}_{dB})_{i,j} = \sigma_{dB}^{(i)}\sigma_{dB}^{(j)}\rho_{dB}^{(i,j)}$ and $(\mathbf{R}_{ss})_{i,j} = \sigma_{ss}^{(i)}\sigma_{ss}^{(j)}\rho_{ss}^{(i,j)}$. We assume that estimates of the shadowing variance and the corresponding fading variance have been obtained according to the method outlined in section IV-B, for both SISO channels i and j. Let us denote by $\rho_{dB}^{(i,j)} \in (-1, 1)$ a trial value of the shadowing correlation. The corresponding fading correlation $\rho_{ss}^{(i,j)}$ that is consistent with the measurements $\{h_i(m), h_j(m), m = 1, ..., M\}$ is determined from

$$(\mathbf{R}_{sh})_{i,j}(\mathbf{R}_{ss})_{i,j} = \frac{1}{M}\sum_{m=1}^{M}h_i(m)h_j^*(m), \qquad (12)$$

where $(\mathbf{R}_{sh})_{i,j} = E[\alpha_{sh,i}\alpha_{sh,j}]$ can be computed from $\sigma_{dB}^{(i)}$, $\sigma_{dB}^{(j)}$ and $\rho_{dB}^{(i,j)}$ [26].

Defining the modeling error $E_2(\rho_{dB}^{(i,j)})$ associated with the trial value $\rho_{dB}^{(i,j)}$ as the average squared error between $ln(BER_{avg,meas}^{(i)})$ and $ln(BER_{avg,th}^{(i)})$, for E_b/N_0 ranging from 0 dB to 5 dB, the shadowing correlation estimate equals the trial value $\rho_{dB}^{(i,j)}$ that minimizes $E_2(\rho_{dB}^{(i,j)})$. Here $BER_{avg,meas}^{(i,j)}$ is the average BER (9) for a 1×2 SIMO transmission involving the channels h_i and h_j, based on the measurements $\{h_i(m), h_j(m), m = 1, ..., M\}$; $BER_{avg,th}^{(i)}$ is the theoretical average BER (7) of a 1×2 SIMO channel described by $\sigma_{dB}^{(i)}$, $\sigma_{dB}^{(j)}$, $\rho_{dB}^{(i,j)}$, $\sigma_{ss}^{(i)}$, $\sigma_{ss}^{(j)}$ and $\rho_{ss}^{(i,j)}$ (which are related by (12)).
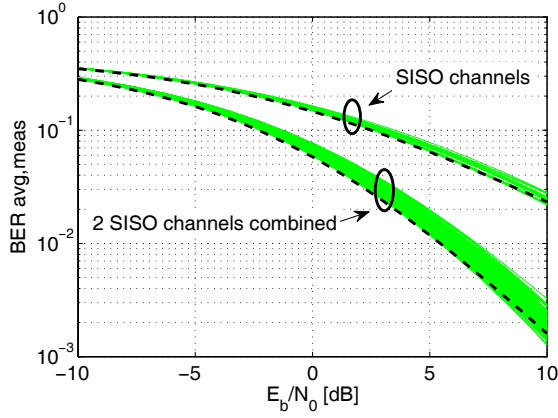
Fig. 4. BER characteristics for the 16 SISO channels and the 120 combinations of 2 SISO channels, compared to i.i.d. Rayleigh fading characteristics of 1st and 2nd order diversity (dashed lines).

TABLE II
AVERAGE CORRELATION COEFFICIENTS FOR THE CASES 1-6.

| | 10λ | | 1.5λ | |
Case	$< \rho_{dB} >$	$< |\rho_{ss}| >$	$< \rho_{dB} >$	$< |\rho_{ss}| >$
1	0.8391	0.0192	1.0000	0.0173
2	0.9141	0.2063	1.0000	0.1008
3	0.0926	0.1120	0.9017	0.1226
4	1.0000	0.1324	1.0000	0.0727
5	0.5022	0.0182	0.9760	0.0189
6	0.5645	0.0852	0.9661	0.0704

V. PHYSICAL INTERPRETATION OF THE SHADOWING CORRELATION COEFFICIENTS

For a number of SISO channel pairs, the averages of the correlation coefficients, estimated according to the previous section, are listed in Table II for the shadowing correlation as well as for the small-scale fading correlation. For the latter, the magnitudes of the complex correlation coefficients are shown. Note that the firefighter is always the receiver and the base station the transmitter.

The following cases are listed:

1) Combination of two SISO channels, received on separate RX antenna patches, transmitted by the same TX antenna patch.
2) Combination of two SISO channels, received on orthogonal polarizations of the same RX antenna patch, transmitted by the same TX antenna patch.
3) Combination of two SISO channels, transmitted on different TX antenna patches, received on the same RX antenna patch.
4) Combination of two SISO channels, transmitted on orthogonal polarizations of the same TX antenna patch, received by the same RX antenna patch.
5) Combination of two SISO channels, not sharing any common antenna patch
6) All 120 possible combinations of two SISO channels.

An interpretation of the correlation values from Table II leads to the following conclusions:

- The shadowing is not significantly decorrelated by polarization diversity (cases 2,4).
- Front-to-back diversity (case 1) also does not significantly decorrelate the shadowing for our measurements. The RX antennas are separated by only a few wavelengths and while the firefighter is walking in the same direction, they are too close to provide substantial decorrelation of the shadowing caused by the environment. For off-body communication, shadowing by the human body [32] is also present and changes according to the orientation of the firefighter. However, in a NLoS situation, with the antennas receiving scattered signals, presumably arriving from many directions, the impact of the orientation on the shadowing correlation factor is limited.
- Using a TX antenna spacing of 10λ provides significant shadowing decorrelation, whereas this is not the case when the spacing is only 1.5λ (case 3).
- The average magnitude of the complex small-scale fading correlation is always low and sometimes slightly higher for cases 2 and 4 (polarization diversity). The maximum value ever occuring for these cases is $|\rho_{ss}| = 0.4052$.

Figure 4 displays (9) for the 16 SISO channels, and for all 120 combinations of two SISO channels. Note that also "artificial" combinations of two SISO channels that do not share any common antenna are included for the sole purpose of estimating the corresponding shadowing and fading correlation coefficients $\rho_{dB}^{(i,j)}$ and $\rho_{ss}^{(i,j)}$.

Observe from Fig. 4 that the BER degradation due to shadowing is often larger for the channel combinations than for the SISO channels. Exploiting the MIMO channel increases the impact of shadowing on the BER curves.

After determining the values of $\sigma_{dB}^{(i)}$ and $\sigma_{ss}^{(i)}$ for all 16 SISO channels and $\rho_{dB}^{(i,j)}$ and $\rho_{ss}^{(i,j)}$ for all 120 combinations of 2 SISO channels, we construct the shadowing correlation matrix (of dimension 16×16) that corresponds to the MIMO setup with 4 transmit and 4 receive antennas, and the shadowing correlation matrices (of dimension 4×4) that correspond to the 36 possible 2×2 MIMO setups.

The fading correlation matrices $\mathbf{R}_{ss}$ can be obtained from the shadowing correlation matrices $\mathbf{R}_{dB}$ according to (2). Often a valid shadowing correlation matrix $\mathbf{R}_{dB}$ is not directly obtained, due to estimation errors. Based on the estimated correlation matrix, which is symmetric but not always positive definite, the nearest valid correlation matrix is obtained using the algorithm of N.J. Higham, documented in [30]. This algorithm is an improvement of the Boyle and Dykstra algorithm described in [31] that was used for shadowing cross-correlation models before in [17], [18]. The resulting corrected matrix is positive definite, as required for the Cholesky decomposition applied in Section III-C. Note that $\mathbf{R}_{ss}$ is recalculated via (2) using the adjusted shadowing correlation matrix.

For 2×2 MIMO links, the estimated shadowing correlation matrix is sometimes positive definite without any adjustment. From our measurements, there is no apparent correspondence between the need for adjusting the correlation matrix and the size of the difference between $BER_{avg,meas}$ and $BER_{avg,th}$. This difference is not smaller for the cases without matrix adjustment.

Fig. 5. BER characteristics for the two 4×4 measurements, with the TX antennas spaced 1.5λ and 10λ apart, versus theoretical BER curves based on the fading and shadowing correlation matrices. The dotted curves represent the theoretical BER for i.i.d. Rayleigh fading channels.

Fig. 6. BER characteristics for measured versus modeled 2×2 MIMO channels for 10λ TX antenna spacing, illustrating the performance of polarization versus spatial diversity. As an indication of the reliability of 2×2 links, the curves for the worst-case antenna combination are included. The dotted curves represent the theoretical BER for i.i.d. Rayleigh fading channels.

VI. MEASURED VERSUS CALCULATED MIMO BER CHARACTERISTICS

The bit error calculations are now applied to the experimental datasets, each containing 2500 measured frames of the 4×4 MIMO link (i.e., 16 SISO channels have been simultaneously measured). The measured set of complex channel gains is also useful for bit error calculations of various 2×2 MIMO systems, obtained by selecting only 2 transmit and 2 receive antennas. The number N of shadowing realizations used in the BER calculation (7) is:

- $N = 10^4$ for the estimation of $\sigma_{\mathrm{dB}}^{(i)}$ values per SISO channel, following the procedure in Section IV-B.
- $N = 10^4$ for the estimation of $\rho^{(i,j)}$ per pair of SISO channels, following the procedure in Section IV-C.
- $N = 10^5$ for the generation of the calculated MIMO BER characteristics (7).

These numbers were chosen experimentally for a good accuracy within a limited calculation time. With the values listed, further multiplying the number of realizations by a factor 10 does not produce a visible difference in the resulting BER curve.

Fig. 5 displays the BER characteristics $BER_{avg,th}$ from (7) and $BER_{avg,meas}$ from (9) for the 4×4 MIMO link, with 2 dual-polarized antenna patches on both sides of the link (TX1-4, RX1-4). TX antenna spacings of 1.5λ and 10λ are considered.

The BER curves related to measurement and model agree very well, with a maximum deviation in E_b/N_0 of only 0.3 dB at $BER = 10^{-3}$. The BER performance of the link improves by 1 dB at $BER = 10^{-3}$ when going from 1.5λ to 10λ transmit antenna spacing. This performance increase is mainly attributed to shadowing decorrelation.

It is interesting to assess the effect of the shadowing correlation on the BER performance. Recalculating the theoretical BER with the shadowing correlation (but not the fading correlation) set to zero produces a deviation (as compared to the BER resulting from the measurements) in E_b/N_0 of about
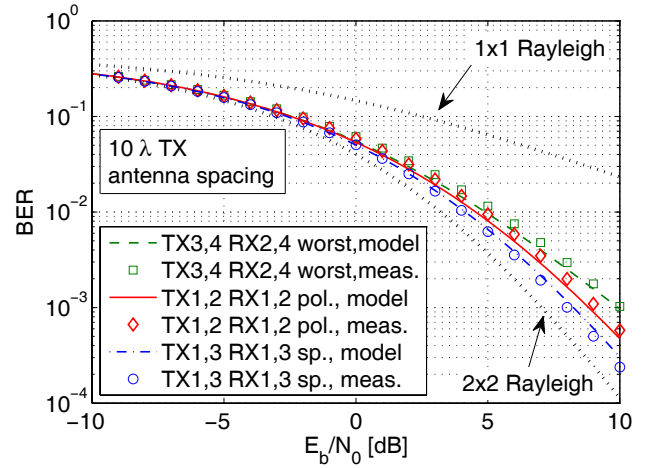
1.4 dB and 0.6 dB at a $BER = 10^{-3}$, for a transmit antenna spacing of 1.5λ and 10λ, respectively, whereas the deviation is only 0.3 dB when accounting for correlated shadowing. This indicates that it is essential to include shadowing correlation into the model to obtain accurate BER results, especially for small antenna spacings.

The 2×2 MIMO links are evaluated by selecting the measurement data corresponding to a combination of two transmit and two receive antenna ports. Fig. 6 illustrates the performance of 2×2 systems, with the TX antennas spaced by 10λ, exploiting either polarization diversity (TX 1 , 2 and RX 1 , 2) or spatial diversity (TX 1 , 3 and RX 1 , 3). The antenna combination that yields the worst-case performance is also included. The worst case corresponds to transmitting with polarization diversity on one antenna patch and receiving front and back with equal polarizations (TX 3 , 4 and RX 2 , 4).

While polarization diversity conveniently only requires one antenna patch at both link ends, the BER performance of spatial diversity is approximately 1 dB better for the higher E_b/N_0 ratios. The curves corresponding to $BER_{avg,th}$ and $BER_{avg,meas}$ agree well, with maximum deviations of about 0.35 dB at $BER = 10^{-3}$.

Figure 6 displays only 3 of the 36 possible signal combinations that compose a 2×2 MIMO link. The accuracy of the model has been assessed for all possible 2×2 MIMO links with 10λ TX antenna spacing. Considering the difference in E_b/N_0 between $BER_{avg,th}$ and $BER_{avg,meas}$, at $BER = 10^{-3}$, for the 36 possible 2×2 MIMO systems, the average and the standard deviation of the modeling errors amounts to 0.0028 dB and 0.21 dB, respectively, which indicates accurate modeling in all cases.

VII. MEASURED VERSUS CALCULATED MIMO CAPACITY

To verify the accuracy of the correlated shadowing and correlated small-scale fading channel model, and to illustrate the suitability of the model for capacity calculations, ergodic channel capacity curves based on both the measurement and
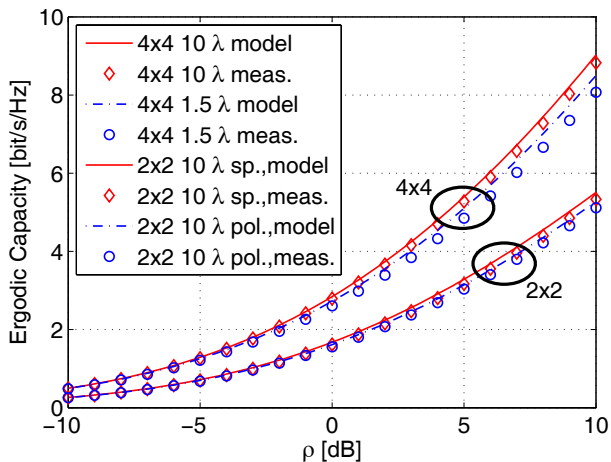
Fig. 7.   Ergodic capacity characteristics for model and measurement for different MIMO orders, transmit antenna spacings and diversity types. Upper set of curves for 4×4 MIMO at 10λ or 1.5λ. Lower set for 2×2 MIMO at 10λ with spatial (sp.) diversity or polarization (pol.) diversity.

the model are compared. Ergodic capacity (in bit/s/Hz) is defined as [35]:

$$\overline{C} = E\left[log_2\left(det\left[\mathbf{I}_{N_R} + \frac{\rho}{N_T}\mathbf{H}\mathbf{H}^H\right]\right)\right], \qquad (13)$$

where ρ is the ratio of total transmit power to noise power, $det(.)$ refers to the determinant, and the expectation $E[.]$ is over the channel statistics. Closed-form expressions for channel capacity in case of correlated Rayleigh fading are documented in [33], [34], although only in case of correlation on one side of the link (either receive or transmit correlation). As we are confronted with both Rayleigh fading and shadowing, and with correlations at both the TX and RX sides, (13) is computed from a simulation of 10^7 realizations of correlated Rayleigh fading with correlated shadowing, according to the parameters from Section IV. Fig. 7 displays a good match of the capacity characteristics (for 10^7 simulated channel realizations) for measurement and model, with a maximum deviation less than 0.6 dB.

VIII. CONCLUSIONS AND REMARKS

Based on channel measurements, a model for the indoor off-body MIMO channel behavior has been derived. This model involves correlated Rayleigh fading and correlated lognormal shadowing with unequal variances. The bit error characteristics and channel capacity curves resulting from the channel measurements are accurately reproduced from the model. The observed deviation in E_b/N_0 at $BER = 10^{-3}$, between the theoretical BER and the BER corresponding to the measurements, is always less than 0.5 dB. The channel capacity curves also match with an accuracy better than 0.6 dB.

The extracted shadowing correlation parameters provide interesting information about the physical channel behavior. In our non line-of-sight environment, for body-worn antennas, shadowing is not significantly decorrelated by polarization diversity or front-to-back diversity. Fixed antennas spaced at

10λ provide significant shadowing decorrelation at the base-station, whereas this is not the case for a spacing of 1.5λ.

Based on the model, the channel behavior extracted from measurements can be reproduced, creating an arbitrary number of measurement-like MIMO channel realizations for simulation purposes. Hence the performance of modulation and channel coding for this indoor off-body MIMO environment can be assessed without performing additional measurements.

The main focus is on the BER as performance indicator, because the relevance of polarization metrics is rather limited in the considered NLoS environment. In order to justify this statement, we have evaluated the XPD and CPR performance indicators for both Line-of-Sight (LoS) and NLoS conditions.

In LoS conditions, with the transmitting and receiving antennas oriented towards each other, high average XPD values up to 9 dB are found, together with low CPR values of around 1 dB. Hence, for this environment, only a small amount of mixing between polarizations occurs.

In the NLoS case, however, the XPD as well as the CPR have average values close to 0 dB with a standard deviation of about 7 dB, indicating the mixing of both polarizations to a variable degree. This is caused by the time-varying channel (motion of people), multipath and scattering in the environment. Additionally, bending of the flexible antennas due to body movements results in a variable distortion of the polarization ellipses. An important factor is also the continuous reorientation of the antennas' main beams due to movements of the rescue worker, causing large variations in momentary XPD as documented in [2].

IX. ACKNOWLEDGEMENTS

REFERENCES

[1] C. Oestges, B. Clerckx, M. Guillaud, and M. Debbah, "Dual-polarized wireless communications: from propagation models to system perfor-mance evaluation," *IEEE Trans. Wireless Commun.*, vol. 7, no. 10, pp. 4019–4031, Oct. 2008.

[2] F. Quitin, C. Oestges, F. Horlin, and P. De Doncker, "Multipolarized MIMO channel characteristics: analytical study and experimental re-sults," *IEEE Trans. Antennas Propag.*, vol. 57, no. 9, pp. 2739–2745, Sep. 2009.

[3] T. Kim, B. Clerckx, D. Love, and S. Kim, "Limited feedback beamform-ing systems in dual-polarized MIMO channel," *IEEE Trans. Wireless Commun.*, vol. 9, no. 11, pp. 3425–3439, Nov. 2010.

[4] RU Nabar, H. Bolcskei, V. Erceg, D. Gesbert, and AJ Paulraj, "Per-formance of multiantenna signaling techniques in the presence of polarization diversity," *IEEE Trans. Signal Process.* (see also *IEEE Trans. Acoustics, Speech, Signal Process.*), vol. 50, no. 10, pp. 2553–2562, Oct. 2002.

[5] V. Erceg, P. Soma, D. S. Baum, and S. Catreux, "Multiple-input multiple-output fixed wireless radio channel measurements and mod-eling using dual-polarized antennas at 2.5 GHz," *IEEE Trans. Wireless Commun.*, vol. 3, no. 6, pp. 2288–2298, Nov. 2004.

[6] R. Parviainen, J. Ylitalo, R. Ekman, P. H. K. Talmola, and E. Huhka, "Measurement based investigations of cross-polarization characteristics originating from radio channel in 500 MHz frequency," in *Proc. 2008 IEEE Antennas Propag. Society International Symp.*, pp. 1–4.

[7] T. F. Kennedy, P. W. Fink, A. W. Chu, N. J. Champagne, G. Y. Lin, and M. A. Khayat, "Body-worn e-textile antennas: the good, the low-mass, and the conformal," *IEEE Trans. Antennas Propag.*, vol. 57, no. 4, pp. 910–918, Apr. 2009.

[8] S. L. Cotton and W. G. Scanlon, "Channel characterization for single- and multiple-antenna wearable systems used for indoor body-to-body communications," *IEEE Trans. Antennas Propag.*, vol. 57, no. 4, pp. 980–990, Apr. 2009.

[9] Y. Ouyang, D. J. Love, and W. J. Chappell, "Body-worn distributed MIMO system," *IEEE Trans. Veh. Technol.*, vol. 58, no. 4, pp. 1752–1765, May 2009.

[10] Y. Ouyang and W. J. Chappell, "Diversity characterization of body-worn textile antenna system at 2.4 GHz," in *Proc. IEEE Antennas Propag. Society International Symp.*, pp. 2117–2120.

[11] A. A. Serra, P. Nepa, G. Manara, and P. S. Hall, "Diversity measurements for on-body communication systems," *IEEE Antennas Wireless Propag. Lett.*, vol. 6, pp. 361–363, Oct. 2007.

[12] I. Khan and P. S. Hall, "Multiple antenna reception at 5.8 and 10 GHz for body-centric wireless communication channels," *IEEE Trans. Antennas Propag.*, vol. 57, no. 1, pp. 248–255, Jan. 2009.

[13] D. Psychoudakis, G. Y. Lee, C.-C. Chen, and J. L. Volakis, "Estimating diversity for body-worn antennas," in *Proc. 2009 European Conf. on Antennas Propag.*, pp. 704–708.

[14] J. Karedal, A. J. Johansson, F. Tufvesson, and A. F. Molisch, "A measurement-based fading model for wireless personal area networks," *IEEE Trans. Wireless Commun.*, vol. 7, no. 11, pp. 4575–4585, Nov. 2008.

[15] B. Clerckx, C. Craeye, D. Vanhoenacker-Janvier, and C. Oestges, "Impact of antenna coupling on 2 x 2 MIMO communications," *IEEE Trans. Veh. Technol.*, vol. 56, no. 3, pp. 1009–1018, May 2007.

[16] M. Hajian, H. Nikookar, F. v. der Zwan, and L. P. Ligthart, "Branch correlation measurements and analysis in an indoor Rayleigh fading channel for polarization diversity using a dual polarized patch antenna," *IEEE Microwave Wireless Components Lett.*, vol. 15, no. 9, pp. 555–557, Sep. 2005.

[17] J. F. Monserrat, R. Fraile, and L. Rubio, "Application of alternating projection method to ensure feasibility of shadowing cross-correlation models," *Electron. Lett.*, vol. 43, no. 13, pp. 724–725, June 2007.

[18] J. F. Monserrat, R. Fraile, D. Calabuig, and N. Cardona, "Complete shadowing modeling and its effect on system level performance evaluation," in *Proc. 2008 IEEE Veh. Technol. Conf.—Spring*, pp. 294–298.

[19] S. S. Szyszkowicz, H. Yanikomeroglu, and J. S. Thompson, "On the feasibility of wireless shadowing correlation models," *IEEE Trans. Veh. Technol.*, vol. 59, no. 9, pp. 4222–4236, Nov. 2010.

[20] N.-R. Jeon, K.-H. Kim, J.-H. Choi, and S.-C. Kim, "A spatial correlation model for shadow fading in indoor multipath propagation," in *Proc. IEEE 2010 Veh. Technol. Conf.—Fall*, pp. 1–6.

[21] R. K. Sharma and J. W. Wallace, "Indoor shadowing correlation measurements for cognitive radio studies," in *Proc. 2009 IEEE Antennas Propag. Society International Symp.*, pp. 1–4.

[22] L. Vallozzi, H. Rogier, and C. Hertleer, "Dual polarized textile patch antenna for integration into protective garments," *IEEE Antennas Wireless Propag. Lett.*, vol. 7, pp. 440–443, May 2008.

[23] P. Van Torre, L. Vallozzi, C. Hertleer, H. Rogier, M. Moeneclaey, and J. Verhaevert, "Indoor off-body wireless MIMO communication with dual polarized textile antennas," *IEEE Trans. Antennas Propag.*, vol. 59, no. 2, pp. 631–642, Feb. 2011.

[24] SM Alamouti, "A simple transmit diversity technique for wireless communications," *IEEE J. Sel. Areas Commun.*, vol. 16, no. 8, pp. 1451–1458, Oct. 1998.

[25] C. Oestges and B. Clerckx, *MIMO Wireless Communications: From Real-World Propagation to Space-Time Code Design*. Academic Press, 2007.

[26] J. G. Proakis *et al.*, *Digital Communication*. Osborne-McGraw-Hill, 2001.

[27] I. M. Kim and D. Kim, "Closed-form exact BER and optimization of generalized orthogonal STBCs," *IEEE Trans. Wireless Commun.*, vol. 7, no. 9, pp. 3323–3328, Sep. 2008.

[28] I.-M. Kim, "Exact BER analysis of OSTBCs in spatially correlated MIMO channels," *IEEE Trans. Commun.*, vol. 54, no. 8, pp. 1365–1373, Aug. 2006.

[29] L. Jacobs and M. Moeneclaey, "BER analysis of square OSTBCs with LMMSE channel estimation in arbitrarily correlated Rayleigh fading channels," *IEEE Commun. Lett.*, vol. 14, no. 7, pp. 626–628, July 2010.

[30] N. J. Higham, "Computing the nearest correlation matrix, a problem from finance," *IMA J. Numerical Analysis*, vol. 22, no. 3, pp. 329–344, 2002.

[31] J. P. Boyle and R. L. Dykstra, "A method for finding projections onto the intersection of convex sets in Hilbert spaces," *Advances Order Restricted Statistical Inference, Lecture Notes Statistics*, vol. 37, pp. 28–47, 1986.

[32] Y. Wang, I. B. Bonev, J. O. Nielsen, I. Z. Kovacs, and G. F. Pedersen, "Characterization of the indoor multiantenna body-to-body radio channel," *IEEE Trans. Antennas Propag.*, vol. 57, no. 4, pp. 972–979, Apr. 2009.

[33] M. Chiani, M. Z. Win, and A. Zanella, "On the capacity of spatially correlated MIMO Rayleigh-fading channels," *IEEE Trans. Inf. Theory*, vol. 49, no. 10, pp. 2363–2371, Oct. 2003.

[34] M. Kang and M. S. Alouini, "Capacity of correlated MIMO Rayleigh channels," *IEEE Trans. Wireless Commun.*, vol. 5, no. 1, pp. 143–155, Jan. 2006.

[35] A. Goldsmith, *Wireless Communications*. Cambridge University Press, 2005.

Patrick Van Torre received the master's degree in Electrical Engineering from Hogeschool Gent, Ghent, Belgium in 1995. For three years he worked as hardware development engineer in the private sector. Since November 1998 he has been active as educator in electronics and researcher in the field of ultrasound technology. He is currently employed by University College Ghent, at the Faculty of Applied Engineering Sciences, where he teaches theory courses in Analog Electronics, organizes project oriented lab sessions and is involved in public relations activities as well as hardware development projects for third parties. He is part-time researcher, affiliated with the Department of Information Technology at Ghent University. His current research focuses on body-worn multiple-input multiple-output wireless communication systems.

Luigi Vallozzi was born in Ortona, Italy, in 1980. He received the Laurea degree in electronic engineering from the Università Politecnica delle Marche, Ancona, Italy, in 2005 and the Ph.D. degree in electrical engineering at Ghent University, Ghent, Belgium, in 2010. He is currently working as a Postdoctoral Research Fellow of the Fund for Scientific Research - Flanders (FWO) within the Electromagnetics Group at the Information Technology Department (INTEC) of Ghent University. His research focuses on design and prototyping of antennas for wearable textile systems, and the modeling and characterization of multiple-input multiple-output wireless communication systems.

Lennert Jacobs (S'07) was born in Ghent, Belgium, in 1983. He received the Diploma degree in electrical engineering in 2006 from Ghent University, Gent, Belgium, where he is currently working toward the Ph.D. degree in the Department of Telecommunications and Information Processing. His main research interests are in error analysis, channel estimation, MIMO techniques, and modulation and coding for wireless digital communications.

Hendrik Rogier was born in 1971. He received the Electrical Engineering and the Ph.D. degrees from Ghent University, Gent, Belgium, in 1994 and in 1999, respectively. He is currently Associate Professor with the Department of Information Technology. From October 2003 to April 2004, he was a Visiting Scientist at the Mobile Communications Group of Vienna University of Technology. He authored and coauthored about 75 papers in international journals and about 100 contributions in conference proceedings. He is serving as a member of the Editorial Boarding of IET Science, Measurement Technology and acts as the URSI Commission B representative for Belgium. His current research interests are the analysis of electromagnetic waveguides, electromagnetic simulation techniques applied to electromagnetic compatibility (EMC) and signal integrity (SI) problems, as well as to indoor propagation and antenna design, and in smart antenna systems for wireless networks. Dr. Rogier was twice awarded the URSI Young Scientist Award, at the 2001 URSI Symposium on Electromagnetic Theory and at the 2002 URSI General Assembly. He is a Senior Member of the IEEE.

Marc Moeneclaey received the diploma of electrical engineering and the Ph.D. degree in electrical engineering from Ghent University, Gent, Belgium, in 1978 and 1983, respectively. He is Professor at the Department of Telecommunications and Information Processing (TELIN), Gent University. His main research interests are in statistical communication theory, (iterative) estimation an detection, carrier and symbol synchronization, bandwidth-efficient modulation and coding, spreadspectrum, satellite and mobile communication. He is the author of more than 400 scientific papers in international journals and conference proceedings. Together with Prof. H. Meyr (RWTH Aachen) and Dr. S. Fechtel (Siemens AG), he co-authors the book Digital communication receivers - Synchronization, channel estimation, and signal processing. (J. Wiley, 1998). He is co-recipient of the Mannesmann Innovations Prize 2000. Since 2002, he has been a Fellow of IEEE. During the period 1992-1994, was Editor for Synchronization, for the IEEE TRANSACTIONS ON COMMUNICATIONS. He served as co-guest editor for special issues of the *Wireless Personal Communications Journal* (on Equalization and Synchronization in Wireless Communications) and the IEEE JOURNAL ON SELECTED AREAS IN COMMUNICATIONS (on Signal Synchronization in Digital Transmission Systems) in 1998 and 2001, respectively.

Jo Verhaevert received the engineering degree and the Ph.D. degree in electronic engineering from the Katholieke Universiteit Leuven, Belgium in 1999 and 2005, respectively. He currently teaches courses on telecommunication at the University College Ghent, Faculty of Applied Engineering Sciences, Ghent, Belgium where he also performs research. His research interests include indoor wireless applications (such as wireless sensor networks), indoor propagation mechanisms and smart antenna systems for wireless systems.